JOURNAL OF PROPULSION AND POWER
Vol. 16, No. 1, January–February 2000

Fuel Injection into a Supersonic Airflow by Means of Pylons

C. Gruenig*
Technical University of Munich, D-85747 Garching, Germany
V. Avrashkov†
Moscow Aviation Institute, RF-125872, Moscow, Russia
and
F. Mayinger‡
Technical University of Munich, D-85747 Garching, Germany

The mixing and reaction processes in a scramjet combustion chamber have been experimentally investigated. Hydrogen was injected into a preheated Mach 2.15 airstream by means of pylon-like fuel injectors. The supersonic flame was stabilized in a purely reaction–kinetical way; i.e., by means of self-ignition. Various pylon designs have been employed to study their influence on fuel mixing and combustion in the supersonic airstream. Based on the results, an optimized fuel injector has been designed and tested. To assess the reacting flow, nonintrusive, optical measurement techniques have been employed: the Rayleigh scattering technique to study the injected mixing jets, and the self-fluorescence of the OH radical to determine location and intensity of the reaction zones. Additionally, the wall static pressure has been measured.

Nomenclature

A	= area
d_{equ}	= equivalent hydraulic diameter
E_{pulse}	= laser pulse energy
G_{mixing}	= mixing efficiency parameter
M	= Mach number
$\dot{m}$	= mass flow rate
n_j	= number of fuel-injection jets
p	= static pressure
p_w	= wall static pressure
p_0	= total pressure
q	= momentum
Re	= Reynolds number
T	= static temperature
T_0	= total temperature
u	= velocity
w	= mass fraction
x	= axial distance from pylon
λ	= wavelength
σ	= scattering cross section
τ	= time scale
Φ	= equivalence ratio

Introduction

THE reacting flow in the combustion chamber of a scramjet propulsion system is characterized by the following:

1) Extremely short residence time of the fluid in the combustor ($\tau_{\text{residence}} = 10^{-4}$–$10^{-3}$ s) because of its very high velocity.

2) The need to optimize total and static pressure, static temperature, and fluid velocity at the combustor exit to allow the high-enthalpy flow to generate a maximum of thrust in the nozzle.

From these characteristics, the requirements of the supersonic mixing and combustion process can be derived:

1) The fuel/air mixing process must occur as rapidly as possible to allow for the shortest possible ignition length; i.e., the distance the fuel is traveling from injection until ignition.

2) The combustion must take place across the whole duct to allow for a wide range of operating equivalence ratios.

3) The fuel/air mixture must react at a sufficiently high rate to release the maximum heat into the flow while it is in the combustor.

The aim of the research activities presented in this paper is to study a combustor concept that satisfies these preceding requirements.

To fulfill the first two requirements, the rapid formation of a homogeneous fuel/air mixture across the whole flow channel is necessary. However, experimental and numerical data show that fuel injection from the wall will result in reaction zones that occupy only a small part of the flow channel.[1–8] Therefore, not all of the oxygen supplied by the airstream entering the combustor can participate in the chemical reactions. Combustor equivalence ratios Φ close to one cannot be achieved, but will be necessary for an optimized trajectory of aerospace planes.[9,10] Furthermore, reaction zones close to the wall will exert excessive thermal loads on the structure of the combustor. Injecting the fuel by means of ramps only partly solves the problem.[11–13] To achieve a satisfactory fuel distribution, pylon-like fuel injectors have been employed. Various pylon designs have been studied with respect to their mixing and combustion performance. Injection parameters studied include injection angle, shape of injection orifice, and number of injection jets. Applying the obtained results, an optimum fuel-injection design has been developed and tested.

Experimental Details

The experimental investigations have been performed at the supersonic test facility of the Institute A for Thermodynamics of the Technical University Munich. A schematic diagram of the test facility is shown in Fig. 1.

An air mass flow of $\dot{m} = 330$ g/s is supplied to the test facility. The total temperature of the airstream is raised to $T_0 = 1350$–1380 K by precombustion of hydrogen in the preheater. To account for the oxygen consumption in the preheater, the airstream is replenished with oxygen ~100 hydraulic diameters upstream of the preheater. Within the laval nozzle, the airflow is accelerated to Mach 2.15. The following summarizes the conditions at the entrance of the supersonic test combustor: $M = 2.15$, $T_0 = 1350$ K, $T = 760$ K, $\dot{m} = 0.33$ kg/s, $p = 1.1$ bar, $u = 1160$ m/s, $Re = 4.6 \times 10^5$, $w_{N_2} = 0.727$, $w_{O_2} = 0.193$, and $w_{H_2O} = 0.08$.

These conditions approximately correspond to flight Mach number $M_0 = 6.5$ at altitude $h = 23.5$ km on a representative trajectory of a transatmospheric accelerator, assuming a typical inlet compression ratio.[14] The composition of the vitiated test air is included in the

Received 21 August 1998; revision received 24 January 1999; accepted for publication 4 February 1999.

*Research Scientist, Institute A for Thermodynamics.
†Senior Scientist, Laboratory of Ramjet Combustion Chamber Testing.
‡Professor, Institute A for Thermodynamics.

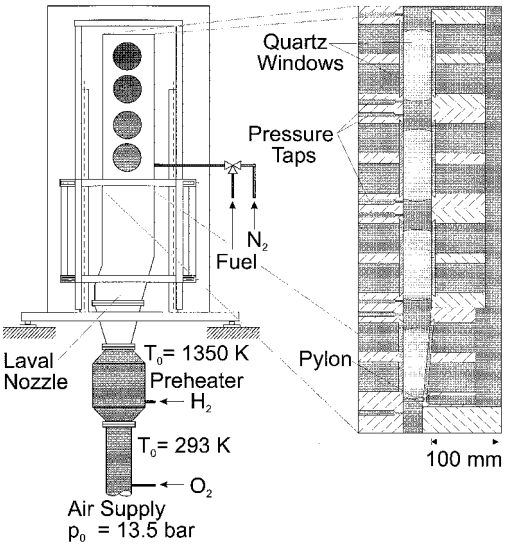

Fig. 1 Supersonic combustion test facility.

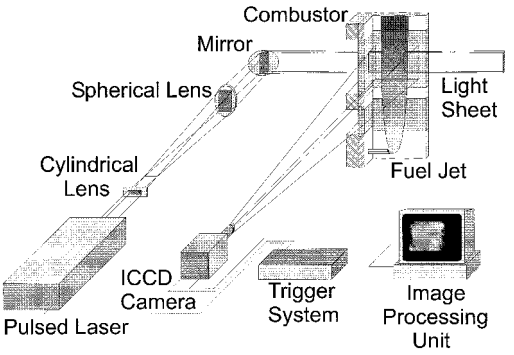

Fig. 2 Optical setup for Rayleigh scattering measurements.

preceding test combuster list. It can be seen that, due to the hydrogen precombustion, there are significant amounts of water. However, for the given combustor pressure range, these concentrations only slightly affect the self-ignition of the fuel.[15,16]

The vitiated, supersonic airstream entering the combustor was checked for contamination with radicals by means of spectroscopic measurements of the OH radical. By this, no radicals could be detected. However, for the given temperature, trace amounts of active radicals cannot be excluded. Nevertheless, this does not question the validity of the test results in general, as those trace amounts of active radicals have been found to have the same effect on the self-ignition performance of a combustor such as a temperature difference of radical-free test air.[16]

The test combustor is of rectangular cross section (27.5 × 25 mm). The overall length is 645 mm. The lower side of the flow channel consists of individual segments allowing for the variation of the combustor area ratio. The expansion angle of 5 deg of the first segment leads to a combustor area ratio $A_{\text{exit}}/A_{\text{entrance}} = 1.48$. The increase of channel area accounts for the fuel input and the heat release of the reaction. The influence of the area ratio onto the supersonic combustion process is known,[17] and, hence, is not a subject of the research work presented. All experiments were conducted with the same combustor area ratio. The fuel is injected at the beginning of the expansion segment.

The combustion chamber is equipped with quartz windows that give optical access into the combustor. To avoid excessive thermal stresses on the quartz windows, the operating times of the combustor were limited to ~10 s.

The combustion tests were performed with constant equivalence ratios Φ, which are defined as

$$\Phi = \frac{(\dot{m}_{\text{fuel}}/\dot{m}_{\text{oxidizer}})}{(\dot{m}_{\text{fuel}}/\dot{m}_{\text{oxidizer}})_{\text{stoichiometric}}} \tag{1}$$

The equivalence ratios were adjusted within the range $\Phi = 0.23$–0.5.

Measurement Techniques

To investigate the mixing and reaction mechanisms in the supersonic flow, nonintrusive, optical measurement techniques have been applied. The employed techniques are only briefly described, and the interested reader is referred to the numerous literature of that field, e.g., Refs. 18–22.

Rayleigh Scattering Technique

To examine the supersonic mixing process, the Rayleigh scattering technique has been employed. Rayleigh scattering is the elastic scattering of light quanta from molecules. Incident laser light excites molecules within the electronic ground state. The excited molecules immediately return to their ground state, spontaneously emitting light. The intensity of the scattering light depends, in part, on the effective scattering cross section $(\mathrm{d}\sigma/\mathrm{d}\Omega)_{\text{eff}}$ of the probed gas mixture. The effective scattering cross section, in turn, depends on the mole fractions x_i of the individual species and their scattering cross sections σ_i. Hence, by choosing gases with different scattering cross sections σ_i, their spatial distribution can be determined.

Helium, with a scattering cross section two orders of magnitude smaller than that of air, has been used to simulate the fuel jets. Additionally, to further increase the contrast of the images, the helium was injected into a cold airflow (low temperature → high number density → higher Rayleigh scattering intensity). To be able to relate these measurement results to the real combustion case, the momentum ratios $q_{\text{air}}/q_{\text{jet}}$ as well as the Reynolds numbers were matched as closely as possible, as will be described later on.

The optical setup for the Rayleigh scattering measurements is shown in Fig. 2. By forming the exciting laser beam ($t_{\text{pulse}} = 17$ ns, $\lambda = 308$ nm, and $E_{\text{pulse}} = 50$ mJ) into a light sheet of 25 × 0.3 mm, spatially and time-resolved images of the two-dimensional distribution of the scattering signal have been recorded. The signal was detected with a 14-bit ICCD camera and processed by an image processing unit.

OH Self-Fluorescence

The emission of self-fluorescence of a flame consists of thermal fluorescence (thermal excitation of the molecules) and chemiluminescence (production of excited molecules by chemical reactions). By choosing a suitable molecule and knowing their role in the chemical kinetics involved, the kinetical processes can be examined.

In the presented work the self-fluorescence of the OH radicals has been selected. The highly reactive OH radicals are products of starting and chain-branching reactions of the hydrogen combustion process, subsequently serve as reaction partners for the exothermic fuel-oxidation reactions, and, are finally consumed by chain-terminating reactions.[23,24] Therefore, the detection of OH self-fluorescence is an appropriate means to determine location and intensity of the reactions zones.

To detect the OH self-fluorescence, the (0, 0) band of the $A^2\Sigma^+ - X^2\Pi$ system (for details about the transitions see Ref. 25) with its bandhead at $\lambda = 306$ nm has been observed by spectrally filtering the flame emission with an interference filter and recording the signal with an intensified charged coupled device camera. The exposure time was set to 0.1 s, which gives averaged images of the reaction zone distribution.

Wall Static Pressure

The static pressure in the reacting flow, which can be measured at the combustor walls, is mainly determined by the heat release of the exothermic reactions. Additionally, the area change of the combustor, the heat transfer to the combustor walls, drag forces in the flow, and the conditions at the combustor entrance and exit also affect the static pressure level. However, assuming that the heat release exerts the primary influence onto the static pressure,

the distribution of the static pressure along the combustor can be regarded as a measure of the heat release into the flow and can be employed to assess the combustion process.

To measure the wall static pressure, seven static pressure orifices are distributed along the upper combustor wall (see Fig. 1).

Principle of Fuel Injection by Pylons

As mentioned earlier, the rapid formation of a homogeneous fuel/air mixture across the whole flow cross section is a prerequisite for compact reaction zones that will result in an efficient scramjet combustor. By injecting the fuel in the center of the flow with pylons, the problem of the slow lateral mass transport in supersonic mixing layers is circumvented. The concept of the fuel injection by pylons is depicted in Fig. 3.

In the upper part of Fig. 3 the fuel distribution with the pylon is shown. Helium was used to simulate the fuel. The mixing jets were visualized with the Rayleigh scattering technique. Multishot images (10 measurements within 0.5 s) display the average shape and development of the injected jets. Measurements were taken along the combustor as well as at selected channel cross sections.

The four separately injected jets are clearly visible. Because of the pressure loss within the strut, the injection pressure at the pylon top is lower than at the bottom injection orifices. Hence, the penetration depth of the jets injected from top holes is reduced as compared with the jets from the pylon base. The fuel rapidly spreads across the channel. 80–100 mm downstream of the pylon, the injected helium has occupied much of the channel cross section, so that fuel self-ignition can take place; compare this with the image in the middle of Fig. 3. The reaction zone takes up another 200-mm axial distance. Only half of the given combustor length is necessary for the fuel/air mixing process, the self-ignition, and the reaction. The whole combustion process can thus be realized within $\sim 10^{-3}$ s.

The measured wall static pressure distribution (the lower part of Fig. 3), reflects the heat release of the combustion. Corresponding to the fast increase of the reaction intensity (compare OH self-fluorescence), the chemical energy of the fuel is quickly transferred to the flow (increase of the wall static pressure). The slight decrease of the wall static pressure toward the combustor exit may be attributed to the heat transfer to the combustor walls. Nevertheless, the supersonic flow exits the combustor in an underexpanded state.

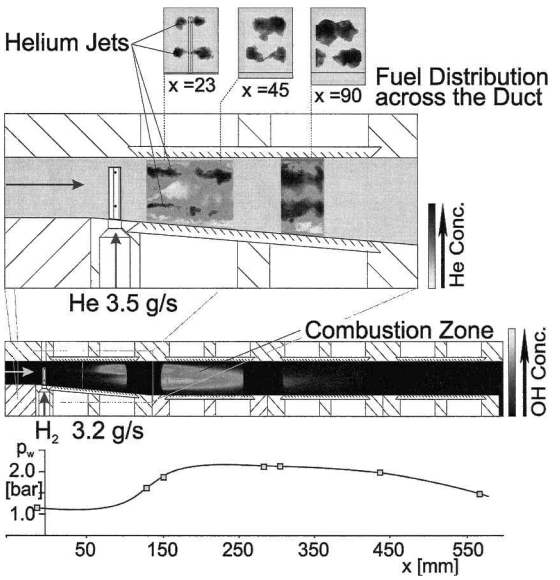

Fig. 3 Fuel injection by pylons: mixing jets visualized with the Rayleigh scattering technique (He injection into unpreheated Mach 2.15 airstream); reaction zones visualized by recording the OH self-fluorescence (H_2 injection into vitiated airstream, $T_{0,air} = 1350$ K); measured wall static pressure.

Comparison of Different Fuel Injectors

Tested Pylon Designs

Various pylon designs have been tested with respect to their mixing and combustion performance. The fuel-injection holes of the pylons were designed to give Mach 1 at the exit; i.e., the holes were of convergent shape. It was not intended to study different fuel Mach numbers and pressures as additional parameters. The orifices were sized to give approximately the same fuel mass flow rate for a selected injection pressure range. The chosen pylon designs are shown in Fig. 4.

These pylons allow the study of the effects of the injection angle, the shape of the injection orifice, and the number of the injected fuel jets; see Table 1, where the injection parameter of the pylons are listed. Pylons A, C, and D inject a single fuel jet; whereas pylon B injects four jets. Pylon A injects normally to the crossflow; whereas the fuel jets of pylons C and D are directed against and with the crossflow, respectively. Pylons A and B inject circular fuel jets, and pylons C and D inject elliptical or slot-shaped fuel jets. Pylon A was later shortened by 2 mm because the original version injected the fuel too close to the opposite combustor wall.

Mixing Efficiency

In the study of the fuel/air mixing process, one can distinguish between large-scale and small-scale mass transport. Large-scale mass transport is based on the action of turbulence, whereas small-scale mass transport basically is the molecular diffusion, which takes place due to concentration gradients. Therefore, the provision of a large fuel/air contact surface, at which molecular diffusion can take place, is a prerequisite for an efficient overall mixing process.

The degree of large-scale mixing can be assessed by Rayleigh scattering measurements, which allow visualization of the concentration profiles at specific flow cross sections. A first, rough estimation of the mixing performance of the different fuel injectors can be obtained. These measurements have been performed for all pylons.

As described before and shown in Fig. 3, helium was injected into an unpreheated airstream to simulate the fuel injection. The flow parameters were adjusted to match the momentum ratio q_{air}/q_{jet} as well as the Reynolds numbers as closely as possible with the original

Table 1 Fuel-injection parameter of the tested pylons

Pylon parameter				Hydrogen flow condition			
Pylon	n_{jet}	Injection angle, deg	Shape of injection hole	d_{equ}, mm	T_0, K	M	v, m/s
A	1	90	Circular	1.58	280	1.0	1160
B	4	90	Circular	0.66	280	1.0	1160
C	1	120	Slot-shaped	1.28	280	1.0	1160
D	1	60	Slot-shaped	1.31	280	1.0	1160

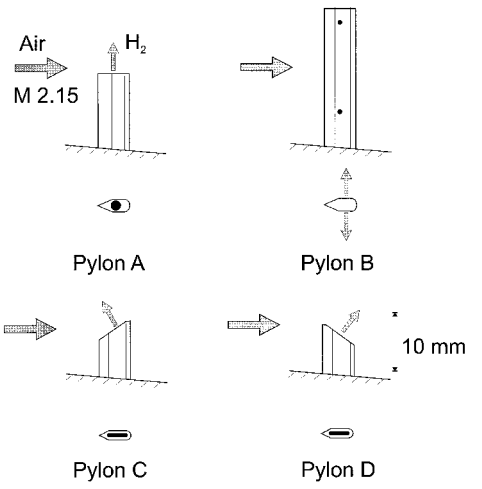

Fig. 4 Various pylon designs tested.

Table 2 Flow parameter of helium injection into cold airstream as compared with hydrogen injection into vitiated airstream

	p_0, bar	T_0, K	M	v, m/s	Re	q_{air}/q_{jet}
Vitiated airstream	7.8	1350	2.15	1190	4.6×10^5	0.176
H_2 jet	39	280	1.0	1160	9.3×10^4	
Unpreheated airstream	4.2	290	2.15	530	2.2×10^6	0.136
He jet	25	280	1.0	850	7.1×10^4	

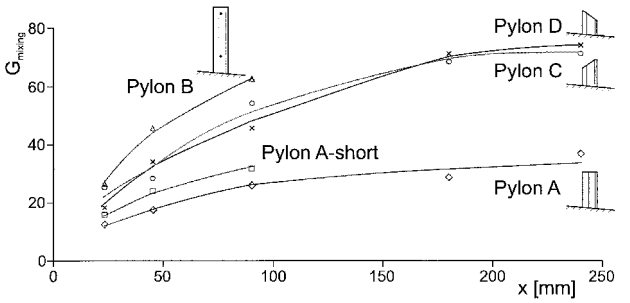

Fig. 5 Mixing efficiency parameter G_{mixing} of the tested pylons plotted against axial distance.

combustion experiment. However, the matching of the momentum ratios has been prioritized. Table 2 summarizes the flow parameter relevant to the comparison of the helium injection into the cold airstream with the hydrogen injection into the vitiated airstream.

It can be seen that the Reynolds numbers of the helium jet and hydrogen jet agree fairly well. However, due to the large difference in the airflow temperature, and, hence, the air viscosity, the Reynolds number of the cold airstream is seven times larger than that of the vitiated airstream. This difference has been accepted to keep the momentum ratios at nearly the same level.

Penetration, location, and spread of the mixing jets have been visualized. The spread of the fuel jets across the channel has been taken as an indicator of the large-scale mixing ability of the different fuel injectors. The injection pressure was held constant for all cases at $p_{inject} = 25$ bar. As pylon A and its shortened version have a larger injection area (see Table 1), and, therefore, inject a higher mass flow rate at the given injection pressure, a mixing efficiency parameter G_{mixing} has been defined as follows:

$$G_{mixing} = \frac{A_{jet}}{\dot{m}_{fuel}} \tag{2}$$

This value can also be interpreted as the inverse of the fuel mass flux. Obviously, the faster the fuel mass flux decreases along the combustor, i.e., as its inverse value increases, the better the mixing process.

In Fig. 5 the mixing efficiency parameter of the various pylons are plotted against the axial distance from the fuel injection. Three conclusions can be drawn:

1) Injection of several fuel jets (such as pylon B) is to be preferred to single jet injection. As several injection jets provide a larger surface area than one single big jet, mixing is most efficient for a number of jets. Additionally, by the injection of several jets, the fuel can be distributed across a large part of the channel right at the injection point (see Fig. 3).

2) Elliptical or slot-shaped fuel jets (pylons C and D) expand faster than circular fuel jets (pylons A and A-short).

3) Different injection angles or opposite orientations of the fuel-injection jets (pylons C and D) do not substantially affect the mixing performance.

Hence, with respect to the large-scale mixing, a number of slot-shaped fuel jets exhibited better performance.

Combustion Performance

The combustion performance of the various fuel-injection configurations has been compared under equal conditions. Table 3 summarizes the airflow conditions at the combustor entrance as well as the fuel-injection parameter.

Table 3 Airflow conditions at combuster entrance and fuel-injection parameter for combustion performance test series

	Pylon	$\dot{m}$, kg/s	M	v, m/s	T_0, K	T, K	p_0, bar	p, bar
Airstream	——	0.33	2.15	1190	1360	765	7.8	1.1
H_2 jet	A	0.0032	1.0	1160	288	150	25.0	13.2
H_2 jet	B	0.0032	1.0	1160	288	150	37.0	19.5
H_2 jet	C	0.0032	1.0	1160	288	150	39.0	20.5
H_2 jet	D	0.0032	1.0	1160	288	150	37.0	19.5

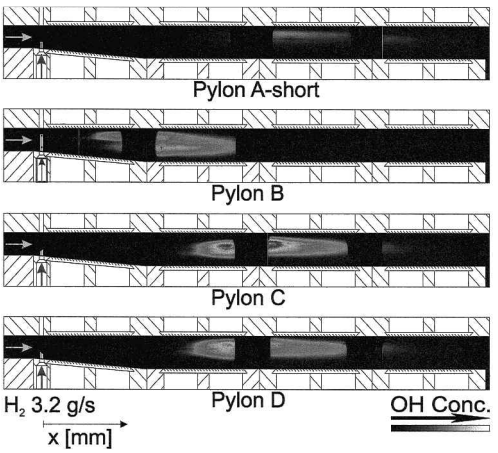

Fig. 6 Reaction zone distributions for the tested fuel-injection pylons (OH self-fluorescence measurements).

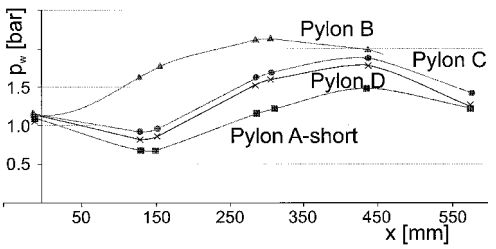

Fig. 7 Static pressure distributions along the upper combustor wall for the tested pylons.

Only the fuel-injection pressure p_{inject} has been varied from pylon to pylon, as the size of the injection orifices slightly differs. By this, equal fuel mass flow rates $\dot{m}_{fuel}$, i.e., equal combustor equivalence ratios Φ, have been ensured.

Extension and intensity of the resultant reaction zones have been determined by recording the OH self-fluorescence. Figure 6 shows the measurement results.

The measured wall static pressures along the combustor, which indicate the heat release rate of the supersonic reaction, are shown in Fig. 7.

Comparing the global combustion performance of the various pylons, it was observed that the combustion performance directly reflects the mixing behavior of the pylon under investigation. Pylon B, showing the most efficient fuel mixing capability, correspondingly shows the best combustion performance: the shortest ignition length, i.e., the axial distance where ignition takes place; a rapid flame development across the flow channel; an early starting heat release into the supersonic flow (rapid increase of the wall pressure); and a short flame length. On the contrary, pylon A, having only low mixing capabilities, shows a correspondingly less-intense combustion.

Pylons C and D show similar locations of the reaction zone. Injecting the fuel against the airflow (pylon C) leads to a higher reaction intensity than injection with the airflow. However, the static pressure distribution indicates only a slight increase of heat release for pylon C.

With regard to the pylon design, the following conclusions can be drawn from the mixing and combustion experiments. Injection of a number of fuel jets provides the most homogeneous fuel distribution across the flow channel. Slot-shaped fuel jets promote a fast fuel–air mixing process.

Furthermore, the mixing and combustion experiments indicate that in a scramjet combustor the overall reaction rate can be actively controlled by the way the fuel is injected. That means that for high-combustor Mach numbers a fuel injector such as pylon B is suitable to keep the supersonic flame sufficiently short ($\tau_{\text{residence}}$ is short, but there is only a low danger of thermally choking the flow). On the other hand, for relatively low combustor Mach numbers, the reaction rate generated by fuel injection with pylon B may be too high, e.g., thermal choking may occur (a variable geometry combustor, which could provide a larger flow area increase to prevent thermal choking, may be undesirable for structural reasons). In this case, a fuel injector with a lower mixing efficiency would be advantageous because the reaction takes place at a lower rate (thus spreading the heat release over a longer axial distance), but it would still have enough time to achieve high-combustion efficiencies due to the longer fuel residence time in the combustor.

Improved Injector Design

Based on the results of the mixing and combustion experiments, the pylon design has been improved. This fuel injector together with the reaction zone achieved with it is shown in Fig. 8.

The pylon basically consists of a strut that is equipped with six small ramps that inject the fuel with a downstream angle of ~30 deg. By means of the six injection orifices, the fuel is spread across the whole duct. To further enhance the mixing, the small ramps could be designed to create vortices in the wake of the ramps.[11] For budget reasons only circular injection orifices could be provided. Nevertheless, the reaction zone achieved with this pylon is very compact and spreads over the whole channel cross section. Ignition takes place only about 50 mm after fuel injection; i.e., it takes only about 10^{-4} s to create a combustible mixture. The main reaction zone is rather short as compared with single-jet pylons (see Fig. 6). The heat release takes place within $\sim 5 \times 10^{-4}$ s. The combustion process finishes well before the combustor exit, indicating a high-combustion efficiency. The test combustor could be shortened (removal of the last segment).

Because only a compact and short supersonic combustor can be used in a real scramjet, the proposed pylon can be regarded as a base concept for a high-performance fuel injector.

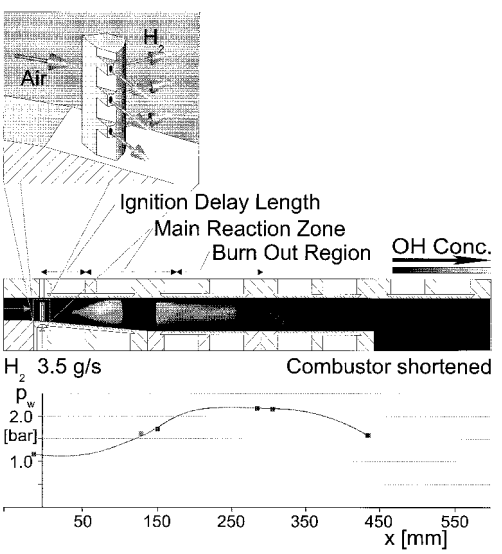

Fig. 8 Optimized pylon and its combustion performance: OH self-fluorescence measurements and wall static pressure distribution.

Conclusions

From the experimental work undertaken, the following conclusions can be drawn:

1) With a suitable injector a homogeneous fuel distribution across the whole combustor cross section can be established. The injection of several fuel jets is to be preferred to single-jet injection. Slot-shaped fuel-injection orifices result in higher mixing efficiencies.

2) The combustion performance of the various pylons directly reflects their mixing ability, i.e., the fuel distribution determines the spread and location of the reaction zone.

3) For the given test facility parameter the supersonic flame could be reduced to ~250 mm. The whole combustion process was finished within about 10^{-3} s.

Acknowledgments

The authors would like to thank the Deutsche Forschungsgemeinschaft for funding these research activities. The project was part of the Sonderforschungsbereich 255 "Hypersonic Transport Systems." The assistance and advice of N. Ardey and W. Gabler (now at Bayrische Motorenwerke Autiongesellschaft, Munich, Germany) is greatly acknowledged. Special thanks goes to the International Association for the Promotion of Co-operation with Scientists from the New Independent States of the Former Soviet Union, Brussels, Belgium; and W. Berry of the European Space Agency/European Space Research and Technology Centre, Noordwijk, The Netherlands, for enabling the stay of V. Avrashkov at the Institute A for Thermodynamics, Technical University of Munich, Germany.

References

[1]Gabler, W., "Gemischbildung, Flammenstabilisierung und Verbrennung in einer gestuften Überschallbrennkammer," Ph.D. Dissertation, Herbert Utz Verlag, Munich, 1996.

[2]Gabler, W., Haibel, M., and Mayinger, F., "Dynamic Structure and Mixing Processes in Sub- and Supersonic Hydrogen/Air Flames in Combustion Chambers with Cascades of Rearward Facing Steps," *Proceedings of the 19th ICAS Congress*, AIAA, Washington, DC, 1994, pp. 1207–1219.

[3]Gabler, W., Haibel, M., and Mayinger, F., "Mixing Process in Reacting and Nonreacting Supersonic Flows," *Proceedings of the 5th European Turbulence Conference* (Siena, Italy), edited by R. Benzi, Kluwer Academic, Dordrecht, The Netherlands, 1995.

[4]Abbitt, J. D., III, Hartfield, R. J., and McDaniel, J. C., "Mole-Fraction Imaging of Transverse Injection in a Ducted Supersonic Flow," *AIAA Journal*, Vol. 29, No. 3, 1991, pp. 431–435.

[5]Yokota, K., and Kaji, S., "Two and Three Dimension Study on Supersonic Flow and Mixing Fields with Hydrogen Injection," AIAA Paper 95-6024, 1995.

[6]Grasso, F., and Magi, V., "Simulation of Transverse Gas Injection in Turbulent Supersonic Air Flows," *AIAA Journal*, Vol. 33, No. 1, 1995, pp. 56–62.

[7]Barber, M. J., Schetz, J. A., and Roe, L. A., "Normal, Sonic Helium Injection Through Wedge-Shaped Orifice into Supersonic Flow," *Journal of Propulsion and Power*, Vol. 13, No. 2, 1997, pp. 257–263.

[8]Karagozian, A. R., Wang, K. C., Le, A.-T., and Smith, O. I., "Transverse Gas Jet Injection Behind a Rearward-Facing Step," *Journal of Propulsion and Power*, Vol. 12, No. 6, 1996, pp. 1129–1136.

[9]Dinkelmann, M., "Reduzierung der thermischen Belastung eines Hyperschallflugzeuges durch optimale Bahnsteuerung," Ph.D. Dissertation, Herbert Utz Verlag, Munich, 1997.

[10]Sachs, G., and Dinkelmann, M., "Trajectory Optimisation for Reducing Coolant Fuel Losses of Aerospace Planes," AIAA Paper 95-3371, 1995.

[11]Donohue, J. M., McDaniel, J. C., and Haj-Hariri, H., "Experimental and Numerical Study of Swept Ramp Injection into a Supersonic Flowfield," *AIAA Journal*, Vol. 32, No. 9, 1994, pp. 1860–1867.

[12]Hönig, R., "Konzentrations- und Temperaturbestimmung in Brennkammern luftatmender Antriebe mit Hilfe laserspektroskopischer Meßverfahren," Ph.D. Dissertation, Technical Univ. of Munich, Garching, Germany, 1995.

[13]Münzberg, H. G., *Flugantriebe*, Springer–Verlag, Berlin, 1972.

[14]Billig, F. S., "Research on Supersonic Combustion," *Journal of Propulsion and Power*, Vol. 9, No. 4, 1996, pp. 499–514.

[15]Mitani, T., "Ignition Problems in Scramjet Testing," *Combustion and Flame*, Vol. 101, 1995, pp. 347–359.

[16]Mitani, T., Hiraiwa, T., Sato, S., Tomioka, S., Kanda, T., and Tani, K., "Comparison of Scramjet Engine Performance in Mach 6 Vitiated and Storage-Heated Air," *Journal of Propulsion and Power*, Vol. 13, No. 5, 1997,

pp. 635–642.

[17]Avrashkov, V., Baranovsky, S., and Levin, V., "Gasdynamic Features of Supersonic Kerosene Combustion in a Model Combustion Chamber," AIAA Paper 90-5268, 1990.

[18]Mayinger, F., *Optical Measurements, Techniques and Application*, Springer–Verlag, Berlin, 1994.

[19]Hauf, W., Grigull, U., and Mayinger, F., *Optische Meβverfahren der Wärme- und Stoffübertragung*, Springer–Verlag, Berlin, 1991.

[20]Haibel, M., Strube, G., and Mayinger, F., "Application of Non-Intrusive Diagnostics Methods to Sub- and Supersonic H_2/Air-Flames," *Proceedings of the 3rd International Symposium on Special Topics in Chemical Propulsion: Non-intrusive Combustion Diagnostics*, edited by U. K. Kuo, Scheveningen, The Netherlands, 1993, pp. 109–112.

[21]Gabler, W., Hönig, R., Lachner, R., Mayinger, F., and Kappler, G., "Spectroscopic Techniques for Ram-Combustors," *Proceedings of the 2nd Space Course*, Vol. 2, No. 20, edited by R. Friedrich, Technical Univ., Munich, 1993, pp. 1–60.

[22]Gabler, W., and Mayinger, F., "Non-Intrusive Laser-Based Optical Measurement Techniques for Reacting and Non-Reacting Supersonic Flows," *Proceedings of the 33rd Aircraft Symposium* (Hiroshima, Japan), 1995, pp. 369–374.

[23]Algermissen, J., and Nötzold, D., "Der zeitliche Ablauf der Verbrennung von Wasserstoff im Überschall-Luftstrom," *Forschung im Ingenieurwesen*, Verein Deutscher Ingenieure Düsseldorf, Vol. 36, No. 6, 1970, pp. 169–200.

[24]Westbrook, C. K., and Dryer, F. L., "Chemical Kinetic Modeling of Hydrocarbon Combustion," *Progress in Energy and Combustion Science*, Vol. 10, 1984, pp. 1–57.

[25]Gaydon, A. G., *The Spectroscopy of Flames*, Chapman & Hall, London, 1974.